

GLOBAL COMPARISON OF THE REGIONAL RAINFALL RESULTS OF ENHANCED GREENHOUSE COUPLED AND MIXED LAYER OCEAN EXPERIMENTS: IMPLICATIONS FOR CLIMATE CHANGE SCENARIO DEVELOPMENT

PETER H. WHETTON, MATTHEW H. ENGLAND¹, SIOBHAN P. O'FARRELL,
IAN G. WATTERSON and A. BARRIE PITTOCK

CSIRO Division of Atmospheric Research, P. B. No. 1, Aspendale 3195, Victoria, Australia; ¹CSIRO Division of Oceanography, G.P.O. Box 1538, Hobart 7001, Tasmania, Australia

Abstract. The extent of agreement amongst current global climate models (GCMs) on the global pattern of rainfall change simulated under enhanced greenhouse conditions is assessed. We consider the results of five experiments which use a simple mixed layer ocean formulation and five which use a fully dynamic ocean model ('coupled experiments'). For many regions of the northern hemisphere there is strong agreement amongst both mixed layer and coupled experiments on the sign of simulated rainfall change. However, in the southern hemisphere there are large, and apparently systematic, differences between the coupled and mixed layer experiments. In particular, whereas the mixed layer experiments agree on simulated rainfall increase in summer in the tropics and subtropics of the Australian sector, the coupled experiments agree (although more weakly) on rainfall decreases. These differences appear to relate to the much reduced warming simulated by the coupled experiments in the high latitudes of the southern hemisphere. However, recent oceanographic evidence suggests that this suppressed warming may be considerably overestimated. We conclude therefore that despite the in-principle advantages of coupled models, it may be too soon to base some regionally specific climate change scenarios solely on the results of coupled experiments.

1. Introduction

The results of global climate models (GCMs) used in enhanced greenhouse experiments are our main source of information on how precipitation may change at the regional scale in response to global warming. However, if some models simulate rainfall increases but others simulate decreases, use of the simulated rainfall changes in regional climate impact studies is problematic. Indeed, the existence of such inconsistency is commonly remarked upon (e.g., Cohen, 1990; Parry et al., 1993), and disagreement on the sign of simulated rainfall change has been demonstrated for some specific regions (e.g., Rowntree, 1990; Grotch and MacCracken, 1991; Burgos et al., 1991). On the other hand, the Intergovernmental Panel on Climate Change (IPCC) surveys of the precipitation results of enhanced greenhouse GCM experiments noted common tendencies for models to increase rainfall in higher latitudes, decrease rainfall over the northern hemisphere mid latitude land areas in summer, and to increase rainfall over South Asia during the south-west monsoon (IPCC, 1990, 1992).

There is also evidence of strong agreement on simulated rainfall change over Australia. Whetton et al. (1993) showed that summer rainfall increases over most

of the continent in each of five recent enhanced greenhouse experiments. There was also considerable agreement amongst the model results in winter, but the pattern of rainfall change was more complicated (regions of increase and regions of decrease). This good agreement amongst models increased confidence in Australian region scenarios of rainfall change constructed from these model results (CIG, 1992; Whetton et al., 1993), and subsequently used in regional climate change impact studies (e.g., Whetton et al., 1993, 1996a; Chiew et al., 1995).

A shortcoming of the work of Whetton et al. (1993) was that it was based on a set of enhanced greenhouse experiments which employed simple mixed layer ocean formulations rather than fully dynamic ocean models. Mixed layer ocean experiments cannot take into account the potential climatic effect of changes in ocean circulation and the transmission of surface warming into the deep ocean. (In the CSIRO regional scenarios, the latter was estimated in a global sense by reference to one-dimensional transient modelling of Wigley and Raper (1992), but potentially important regional variations were ignored). The results from a number of enhanced greenhouse experiments with coupled ocean-atmosphere models are now available. These experiments employ general circulation models of the ocean and thus they can simulate the pattern of uptake of greenhouse warming by the deep ocean and changes in ocean circulation. These models also simulate a pattern of global warming which is rather different to that simulated in the mixed layer experiments. The main difference is much weaker warming in the mid to high latitudes of the southern hemisphere and in the north Atlantic (IPCC, 1992). This change in the pattern of warming may be expected to lead to different patterns of simulated rainfall change in some regions.

Here we scrutinise the global patterns of simulated rainfall change in ten recent enhanced greenhouse experiments, five of which use a mixed layer ocean (the 'mixed layer experiments') and five of which use full ocean models (the 'coupled experiments'). We assess the extent of agreement amongst models on the direction of simulated rainfall change at the regional scale, and note that there are significant (and apparently systematic) differences between the mixed layer and coupled experiments. (Our approach is similar to that used by Kellogg and Zhao (1988) and Zhao and Kellogg (1988) when they assessed agreement amongst models in simulated change in regional soil moisture). Apparent links between the patterns of simulated rainfall change and those of temperature are identified. Results for the Australian region are examined in greater detail using the coupled and mixed layer rainfall results of the same version of the CSIRO GCM. As well as being of particular interest to Australian climate-change studies, it will be seen that this region is where differences in simulated rainfall change between coupled and mixed layer experiments are the greatest. The implications of these results for rainfall scenario development are then assessed with reference to oceanographic evidence on the reliability of current coupled models in the southern hemisphere.

Table I
Details of the mixed layer experiments used

Experiment acronym	Reference	Horizontal resolution (number of waves or lat. \times long.)	Number of years of data used for the 1 \times CO ₂ and 2 \times CO ₂ means
BMRCM	Colman et al. (1994)	R21	14
CCCM	McFarlane et al. (1992)	T32	20
CSIROM	Watterson et al. (1995)	R21	30
GFDLM	IPCC (1990)	R30	10
UKMOM	Gregory and Mitchell (1995)	2.5° \times 3.75°	10

2. Details of GCM Experiments Used

The analysis presented here uses the results of enhanced greenhouse experiments conducted with models from a range of research centres: CSIRO, the Australian Bureau of Meteorology Research Centre (BMRC); the United Kingdom Meteorological Office (UKMO), the Geophysical Fluid Dynamics Laboratory (GFDL), the Canadian Climate Centre (CCC) and the Max Planck Institute, Hamburg (MPI). Details of the experiments, which include both mixed layer and coupled experiments are set out in Tables I and II. For all experiments, precipitation and surface temperature output are used, and for the CSIRO experiments mean sea level (MSL) pressure and 807 hPa winds are also used.

All the mixed layer experiments (BMRCM, CCCM, CSIROM, GFDLM, UKMOM) used a simple mixed layer ocean without ocean currents, but with a prescribed heat flux (' Q -flux') within the ocean layer which compensates for the absence of currents under present climate conditions. The experiments were run to equilibrium for 1 \times CO₂ and 2 \times CO₂ conditions. The results considered here are based on at least 10 years of post-equilibrium simulated data for each run. All the coupled experiments (CSIROC, GFDLC, MPILC, MPIOC, UKMOC) used an atmospheric model coupled to a full ocean model with a flux correction (which reduces climate drift). They were run under a scenario of 1% per annum compounding increase in CO₂ concentration out to at least just beyond the time of CO₂ doubling and under control conditions for a similar duration. The results considered here are based on at least 10 years of simulated data at or near the time of CO₂ doubling, referenced to the corresponding period of the control run (except in the GFDLC experiment, where the reference was the full 100 years of the control run). For each model we would have liked ideally to have used a thirty-year sample from the enhanced greenhouse run centred at the time of CO₂ doubling referenced to the corresponding thirty years of the control run, but we were restricted by the form in which data were available to us. Some further information on these experiments can be found amongst the references in the table. The current version of the CSIRO

Table II

Details of the coupled experiments used. In the enhanced greenhouse runs, each model used a 1% per annum (compounding) increase in CO₂ concentration

Experiment acronym	Horizontal resolution (number of waves or lat. × long.)	Reference	Years of data used in enhanced greenhouse means	Years of data used in control means
CSIROC	R21	Gordon and O'Farrell (1996)	30 years centred ten years before CO ₂ doubling	Corresponding 30 years of control run
GFDLC	R15	Manabe et al. (1991)	20 years centred at doubling	Full 100 years of control run
MPILC	T21	Cubasch et al. (1992)	10 years centred at doubling	Corresponding 10 years of control run
MPIOC	T21	Lunkeit et al. (1994)	10 years centred at doubling	Corresponding 10 years of control run
UKMOC	2.5° × 3.75°	Murphy (1995) and Murphy and Mitchell (1995)	10 years centred at doubling	Corresponding 10 years of control run

model (CSIRO Mk 2) differs from that described in Watterson et al. (1995) mainly through the inclusion of a new soil/canopy scheme (Kowalczyk et al., 1991), sea ice scheme (O'Farrell, 1996) and improved moisture transport scheme. For use in our analysis here, all the model results were interpolated to a common grid of 3.2° latitude by 5.6° longitude.

Although the experiments used cannot be considered fully independent of one another, no two are closely related. In all but one case, the experiments differ from one another either due to differences in the formulations of the models of the various research centres (although some parameterisation schemes are common to a number of models), or the use of the coupled, rather than mixed layer, ocean formulation. The two coupled experiments of MPI have substantially different ocean models and slightly different atmospheric models (see references in table). Some additional recent mixed layer experiments were available to us, but were excluded because either they were undertaken with older versions of the models already represented or did not use a Q -flux. We excluded the one additional coupled experiment for which we had data (that of Washington and Meehl, 1989), primarily because it did not use a flux correction. Climate models that do not use this correction term drift away from a realistic simulation of the present-day climate (the tropics usually become too cool and the high latitudes too warm). Including a non-flux-corrected model in a grouping of mainly flux-corrected models would have made the statistical analysis to be undertaken here problematic. See also Whetton et al. (1996b).

Table III

Pattern correlation coefficients for GCM-simulated precipitation versus observed data. The observations are those of Legates and Willmott (1990). The domain used is the globe north of 40° S, and a latitude-dependent area weighting is applied. The high latitudes of the southern hemisphere are excluded because observations over the ocean in that zone are of limited reliability (see Whetton, 1996). The closer the pattern correlation coefficient is to one, the better is the GCM simulation of the spatial pattern of precipitation

Mixed layer models	DJF	JJA	Coupled models	DJF	JJA
BMRCM	0.63	0.57	CSIROC	0.74	0.66
CCCM	0.63	0.54	GFDLC	0.66	0.55
CSIROM	0.74	0.65	MPILC	0.66	0.65
GFDLM	0.56	0.53	MPIOC	0.73	0.71
UKMOM	0.68	0.65	UKMOC	0.76	0.69

It should be noted that none of the enhanced greenhouse experiments analysed here include anthropogenic sulphate aerosol forcing. Any future increase in this forcing is expected to have a cooling effect on climate, but predominantly in parts of the northern hemisphere close to the major source regions (Charlson et al., 1991; Taylor and Penner, 1994, Mitchell et al., 1995). It could be expected that simulated patterns of precipitation change for enhanced greenhouse conditions would also be affected by the inclusion of sulphate aerosols. However, the climatic effect of aerosols are likely to be less important in the southern hemisphere where sulphur emissions and concentrations of aerosols are relatively low.

The pattern correlation results presented in Table III provide an indication of how well observed precipitation is simulated under $1 \times \text{CO}_2$ conditions in the GCM experiments considered here. Given that the current study is based on a comparison of the spatial pattern of simulated precipitation change from a range of GCMs, a statistic which tests the model's simulation of the spatial pattern of observed precipitation was considered most appropriate. The range of pattern correlation values (0.53–0.76) indicate that the main features of the observed seasonal patterns of precipitation are captured by all of the GCMs used. Some further global validation information may be found amongst the references given in Tables I and II. Whetton et al. (1996b) discusses the control performances in the southern hemisphere of most of the GCM experiments considered here. Note also that validation studies of both the atmospheric and oceanic results of current coupled GCMs will form an important component of the incipient Coupled Model Intercomparison Project (CMIP) (see CLIVAR, 1995).

3. Regional Rainfall Change: Mixed Layer Versus Coupled GCM Results

For the periods December to February (DJF) and June to August (JJA), global maps of simulated rainfall change (enhanced greenhouse conditions relative to control conditions) for each of the five mixed layer experiments are interpolated to a common grid, and at each grid point the number of the models which showed a rainfall increase is counted. DJF and JJA maps of this count are shown in Figure 1 for the mixed layer experiments, and Figure 2 shows the corresponding results for the five coupled experiments. The results are then analysed further to compare the extent of agreement amongst models to that expected by chance. Figure 3 shows a graph, for each season and model grouping, of the frequency of grid point counts in each of the six classes (model counts of zero through to five) compared to the expected chance frequency. (To reduce the bias towards the high latitudes, where the density of grid points is highest, Figure 3 uses the restricted domain of 60° S to 60° N.) The expected frequency is calculated using binomial probability theory given knowledge of the proportion of grid points with increases in each model over the domain considered (examples of the calculation are given in the figure caption). Using the actual proportion of increases in each model (rather than assuming increases and decreases equally likely) means that differences of the simulated frequencies from the expected frequencies do not arise simply from the the global tendency for the models to simulate increased precipitation. (Note that no assessment is given here as to whether differences between expected and actual frequencies in Figure 3 are statistically significant. The need to deal with spatial autocorrelation, which varies between models and spatially within models, makes such an assessment far from trivial, and we have not as yet found a satisfactory approach.)

There is good agreement in the simulated sign of rainfall change in the mixed layer ocean experiments over several broad regions (Figure 1). In particular, throughout most of the high latitudes (and extending to the mid latitudes in the winter hemisphere) rainfall increases in all models. Models tend to increase rainfall in the inter-tropical convergence zone in general and in the summer monsoon regions in particular. Rainfall increases in the equatorial Pacific in both seasons, and south Asia in JJA, and across eastern Africa, the Indian Ocean just south of the equator and over northern Australia in DJF. Models agree on decreases over the mid latitude land areas of the northern hemisphere in summer (particularly North America and southern Europe). The mixed layer models all show increases over Australia in DJF and over southernmost parts of Australia in JJA. Models agree on decreases over much of southern inland Australia in JJA. Figure 3 shows that the frequencies of counts at a grid point of 0 and 1 (agreement on decreasing rainfall) and 5 (strong agreement on increasing rainfall) are considerably greater than the corresponding chance frequency.

There is also considerable agreement amongst the coupled models on the sign of the simulated rainfall change (Figure 2). For the northern hemisphere, the pattern

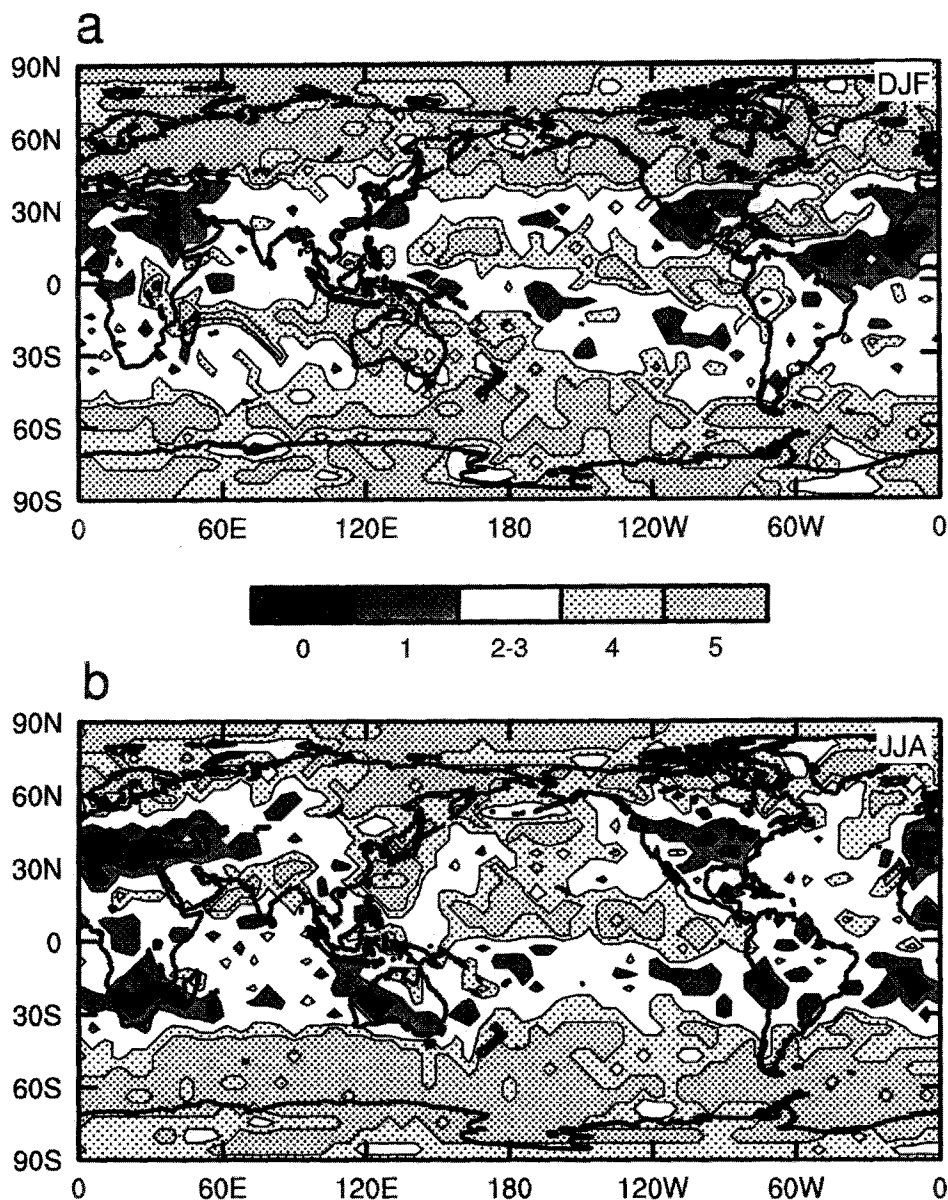


Figure 1. Grid point by grid point counts of the number of models simulating a rainfall increase using the five mixed layer experiments: (a) DJF, (b) JJA.

is very similar to that obtained with the mixed layer ocean experiments, and thus confidence in the simulated pattern of change is increased. By contrast the pattern in the southern hemisphere is considerably different. In DJF, the coupled models show marked areas of decreasing rainfall in mid latitudes, particularly over or near the continents, whereas the mixed layer ocean experiments showed more limited

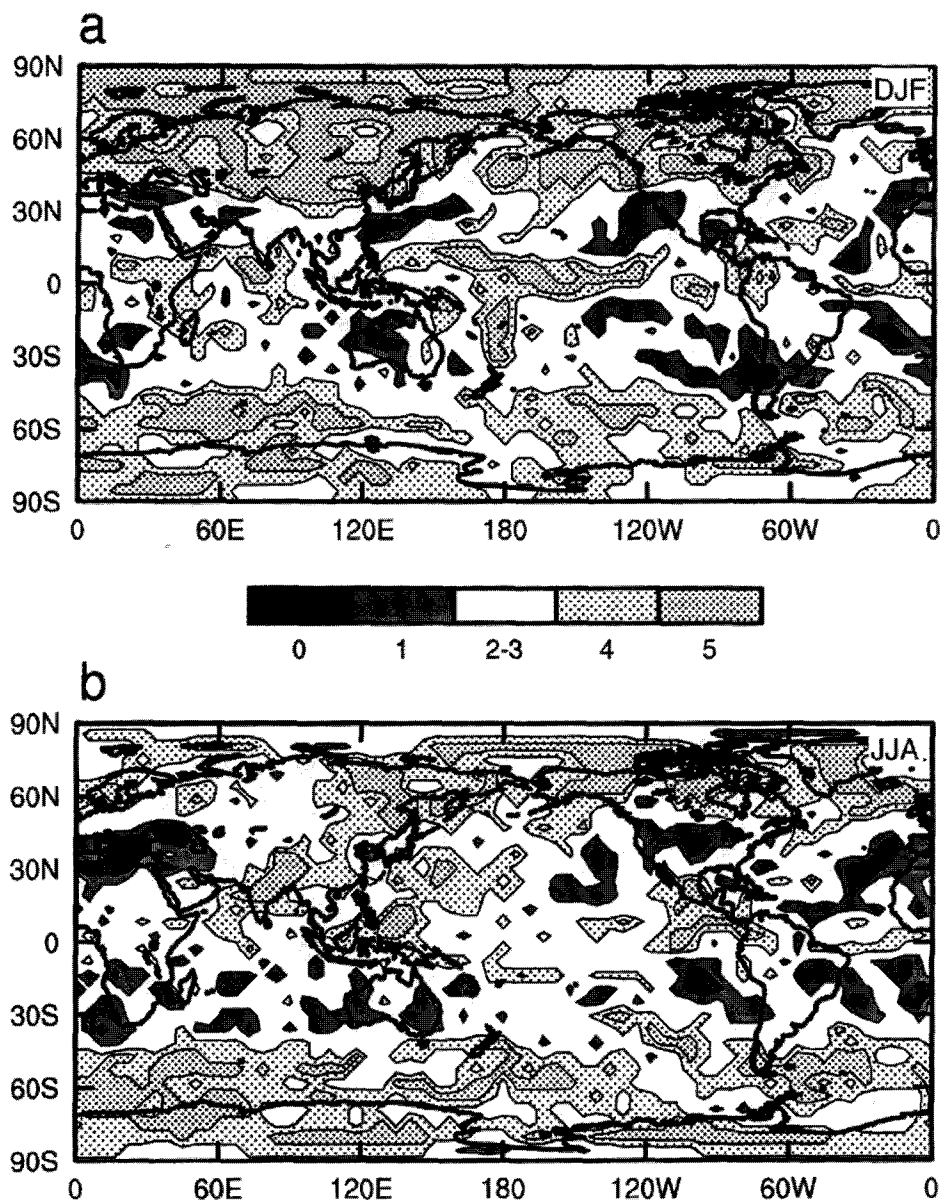


Figure 2. As Figure 1, but for the five coupled experiments.

regions of rainfall decrease. The differences are most striking in the Australian sector, as clearly evident when the difference between the coupled and mixed layer results are mapped (Figure 4). The agreement on DJF rainfall increase over much of the tropics and subtropics of the Australian sector seen in the mixed layer ocean experiments is absent in the coupled experiments where some agreement on rainfall

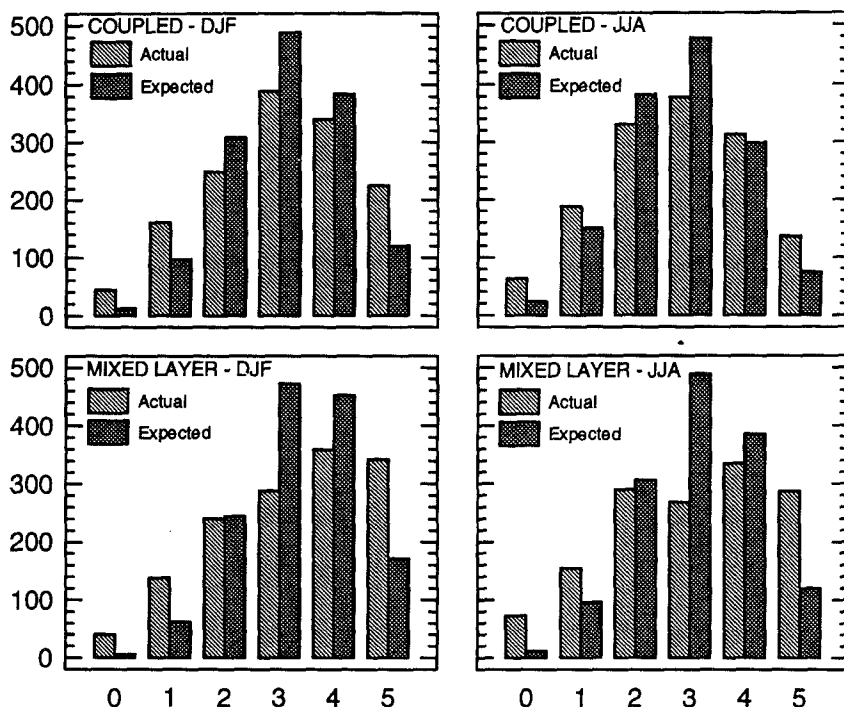


Figure 3. Frequency of model agreement counts of 0–5 obtained for the GCM results ('actual') and as would be expected by chance ('expected') for the domain 60° S–60° N. Separate results are shown for the mixed layer and the coupled experiments, and for DJF and JJA. Calculation of the expected frequency for the domain follows standard binomial probability theory, except that allowance is made for the variation from model to model in the probability of increase (the proportion of grid points showing simulated increases for an individual model). For example, to obtain the expected fraction of grid points showing a count of five, the product of each of the probabilities of increase for the five models is calculated. Multiplying the result by the total number of grid points then gives the expected frequency. A similar calculation using the probabilities of decrease (complementary to those of increase) for each of the five models provides the expected frequency of a zero count. Frequencies for the intermediate counts (1–4) are calculated by allowing for all relevant combinations of the models.

decrease is now evident. In both seasons, but particularly in JJA, the agreement of rainfall increase in the mid to high latitudes of the southern hemisphere seen in the mixed layer ocean experiments is much weaker in the coupled experiments (see Figure 4).

In general, agreement amongst models appears a little weaker than it was in the mixed layer ocean experiments, although the extent of agreement expected by chance is also decreased (this change is most evident in the '5 out of 5' category in Figure 3). This may be related to the fact that the coupled experiments show global warmings around half of those of the mixed layer ocean experiments (this is because the coupled enhanced greenhouse experiments are not at equilibrium and are affected by the thermal inertia of the ocean). This weaker greenhouse signal

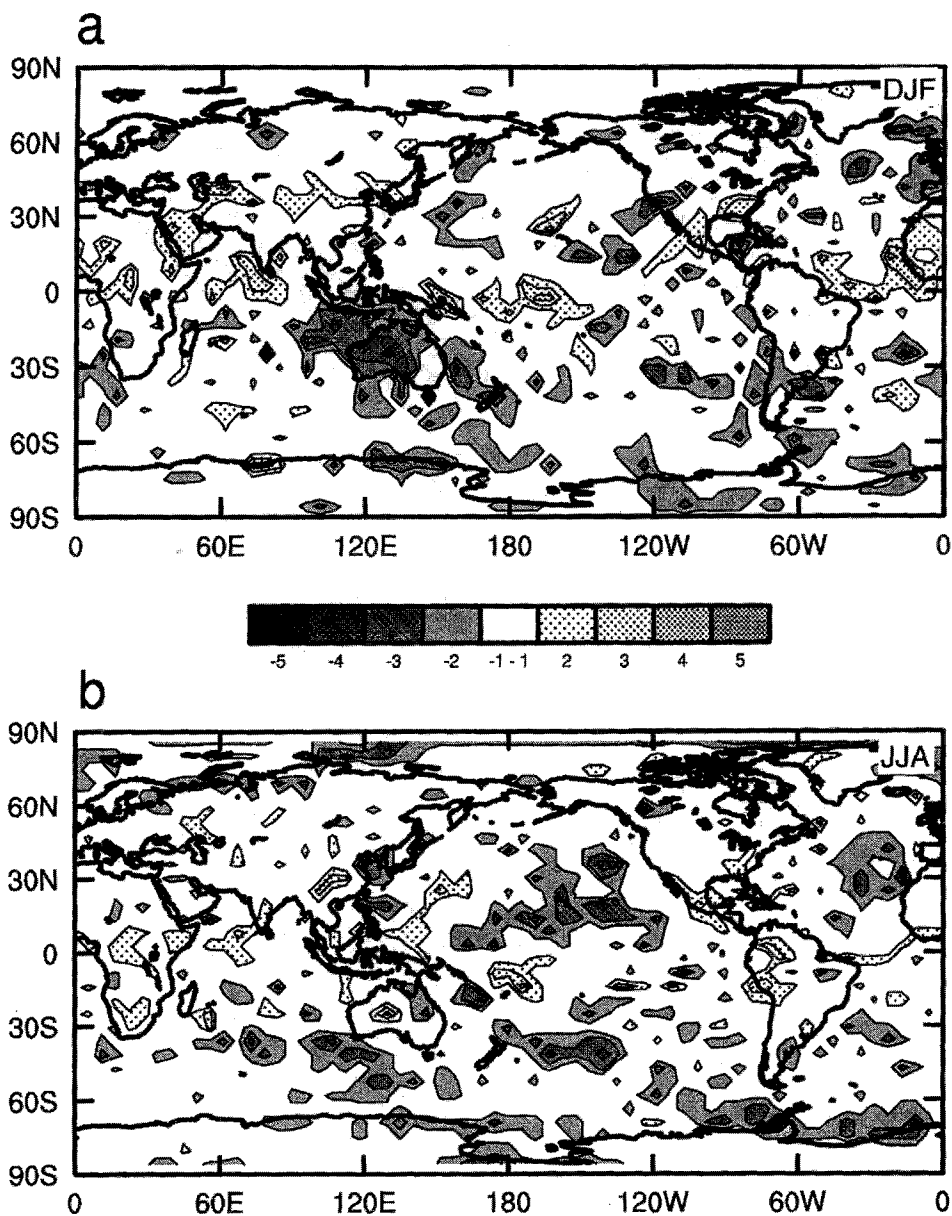


Figure 4. Difference in rainfall increase count between coupled and slab ocean experiments: (a) DJF (difference between Figure 1a and Figure 2a), (b) JJA (difference between Figure 1b and Figure 2b).

would be expected to reduce the signal-to-noise ratio in the coupled experiments relative to the mixed layer experiments. With reduced signal-to-noise, agreement amongst models on the sign of rainfall change can be expected to be weaker.

4. Why Are the Rainfall Results of the Coupled Models Different in the Southern Hemisphere?

It has been recognised for some time (e.g., IPCC, 1992) that the coupled experiments differ from the mixed layer ocean experiments significantly in the global pattern of warming they simulate. In the mixed layer experiments warming is greatest in the high latitudes of both hemispheres, whereas in the coupled experiments warming is suppressed over the far north Atlantic, and throughout the high latitudes of the southern hemisphere (where in certain experiments cooling can even occur). This is due to the coupled models simulating deep vertical mixing in these oceanic regions (which the mixed layer oceans cannot simulate). This mixing transports heat to depth and delays the surface warming. Figure 5 shows zonal averages profiles of annual mean (DJF and JJA) warming (normalised to a global annual warming of one degree) for the mixed layer and coupled experiments used here. (Normalisation removes variation due to the differing global climate sensitivities of the various models.) The figure clearly shows how the difference in the warming pattern is most marked in the southern hemisphere. Notably, the differences between the coupled and mixed layer meridional profiles of warming are not confined to the high latitudes of the southern hemisphere but extend, in a more subtle form, through the subtropics and tropics. In particular, warming averaged over the five mixed layer experiments increases between the equator and 30° S, whereas when averaged over the five coupled models it varies little over this latitude range.

On the broadest scale, the large hemispheric imbalance in the warming in the coupled models can be expected to lead to a similar imbalance in rainfall change (see Murphy and Mitchell, 1995). In the absence of other changes, greater warming would be expected to lead to greater increases in evaporation and hence in rainfall. Averaged over the mixed layer experiments considered here, annual mean area-averaged warming is 8% larger in the northern hemisphere relative to the south, whereas it is 56% larger in the coupled experiments. The corresponding results for average percentage rainfall change are 41% and 126%. The relatively smaller average rainfall increase in the southern hemisphere in the coupled case would contribute to poorer agreement amongst these models on rainfall increase, as is generally evident in that hemisphere. It is less clear why the most marked difference between the simulated rainfall changes of the coupled and mixed layer experiments should occur in the tropics and subtropics of the Australian sector. However, it could be expected that the warming profile (Figure 5) in the mixed layer experiments, but not that in the coupled experiments, would enhance the southward movement of the heat equator, and hence the intertropical convergence zone and the monsoons, in the southern summer.

Rainfall changes in the Australian sector are investigated further with reference to differences in the pattern of temperature, wind and pressure change as simulated by the CSIRO coupled and mixed layer experiments. It was for only these two experiments that we had the wind data (needed for examining changes in

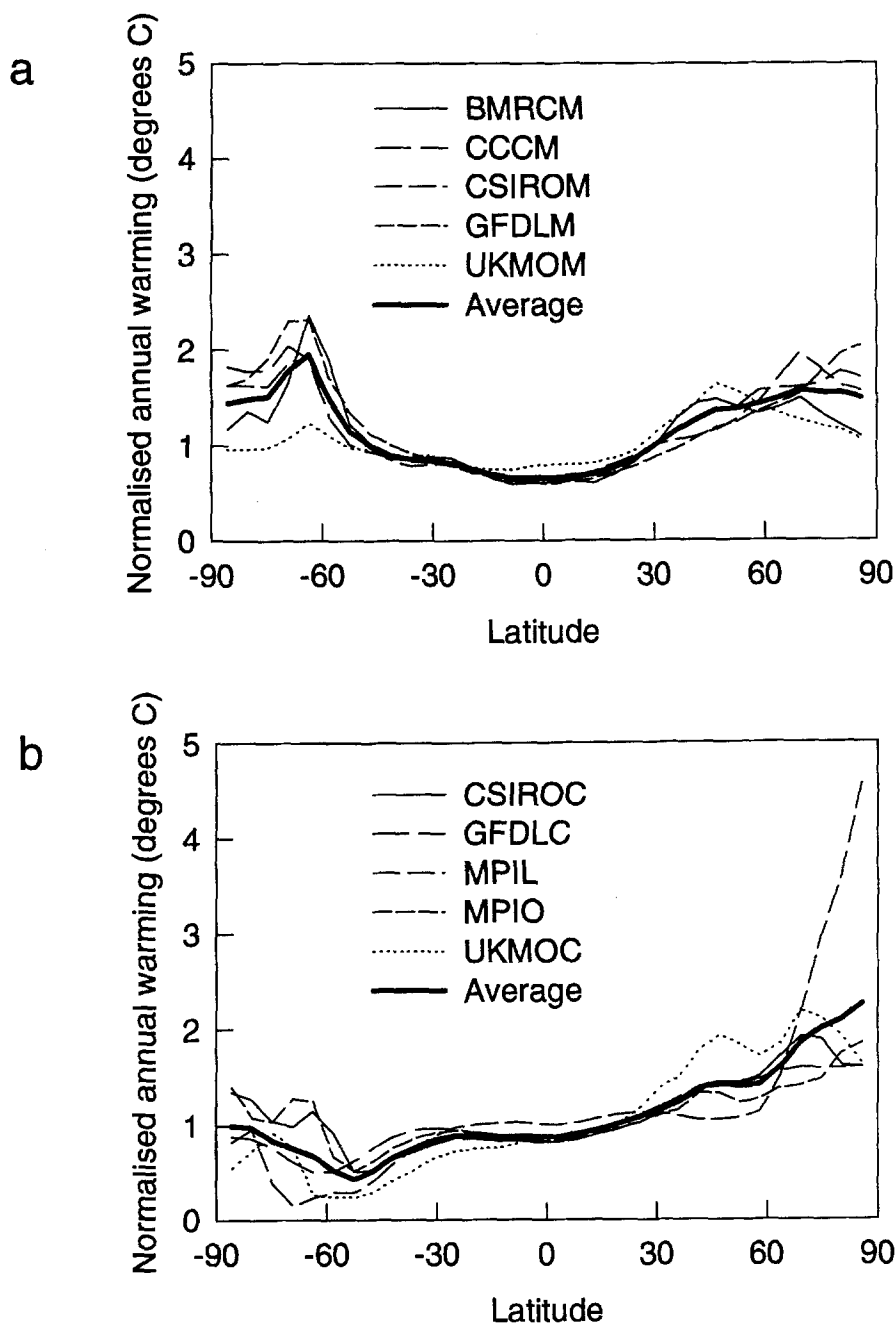


Figure 5. Zonal averages of normalised annual warming in (a) each of the mixed layer experiments and the average of the five and (b) in each of the coupled experiments and the average of the five. All the warming curves are normalised to a global average warming of one degree Celsius.

atmospheric dynamics), but this pair of experiments also has the advantage of being run with the same atmospheric model. The difference between simulated rainfall change for DJF in the CSIRO-M and CSIRO-C simulations is shown in Figure 6a, and corresponding analyses for vector wind, temperature and MSL pressure are shown in Figures 6b–d. In each case, the patterns of change were normalised to that for one degree of global warming before the difference was calculated. Normalisation ensures that the globally weaker greenhouse signal of the coupled models does not affect the calculated differences. (Note that if one ignores minor differences in the control runs of the two experiments the maps in Figure 6 can be viewed as the difference between the enhanced greenhouse runs of the coupled and mixed layer ocean models).

Figure 6a shows marked differences in simulated rainfall change over northern and western Australia and over a large area to the north-west of the continent. Consistent with the results seen with the full set of models (Figures 1 and 2), the enhanced greenhouse coupled climate is substantially drier than the mixed layer climate. A major area of anomalous easterly winds in the coupled enhanced greenhouse run extends through the area of reduced rainfall (Figure 6b). As the prevailing winds in this region are the monsoonal north-westerlies, the wind anomaly in Figure 6b represents a weakening of these winds in the coupled enhanced greenhouse experiment relative to the mixed layer experiment. (Indeed, relative to control conditions these monsoonal winds weaken in the coupled experiment but strengthen in the mixed layer experiment – analysis not shown). It is to be expected that a weakening of the monsoonal westerlies should be associated with a rainfall decrease in the region.

The wind anomaly in Figure 6b reflects a general tendency around the hemisphere for a low latitude easterly wind anomaly in the coupled experiment relative to the mixed layer experiment (Figure 7). Indeed, the coupled enhanced greenhouse experiment has a more vigorous zonal circulation in general (including stronger mid latitude westerlies) as a result of its steeper north to south temperature gradient. However, there is also a suggestion that the regional pattern of warming in the coupled enhanced greenhouse experiment, relative to the mixed layer experiment, may also be contributing directly to the low latitude wind anomaly. The regional difference in normalised warming (Figure 6c) shows the suppressed warming of the coupled run (negative values in the figure) south of around 40° S. However, this relatively cooler water in the coupled greenhouse run extends as far north as 10° S to the west of Australia, possibly due to transport by the Indian Ocean Gyre. Such a cool sea surface temperature anomaly in the subtropics can be expected to lead to a local positive pressure anomaly, which is indeed evident in the MSL pressure analysis (Figure 6d). This pressure anomaly would in turn enhance easterly flow on its northward margin consistent with the wind anomaly seen in Figure 6b.

Observed variations in Australian DJF rainfall and eastern Indian Ocean pressure and winds are related in a manner similar to that suggested by Figure 6, although these relationships form part of a broader pattern dominated by El Niño Southern

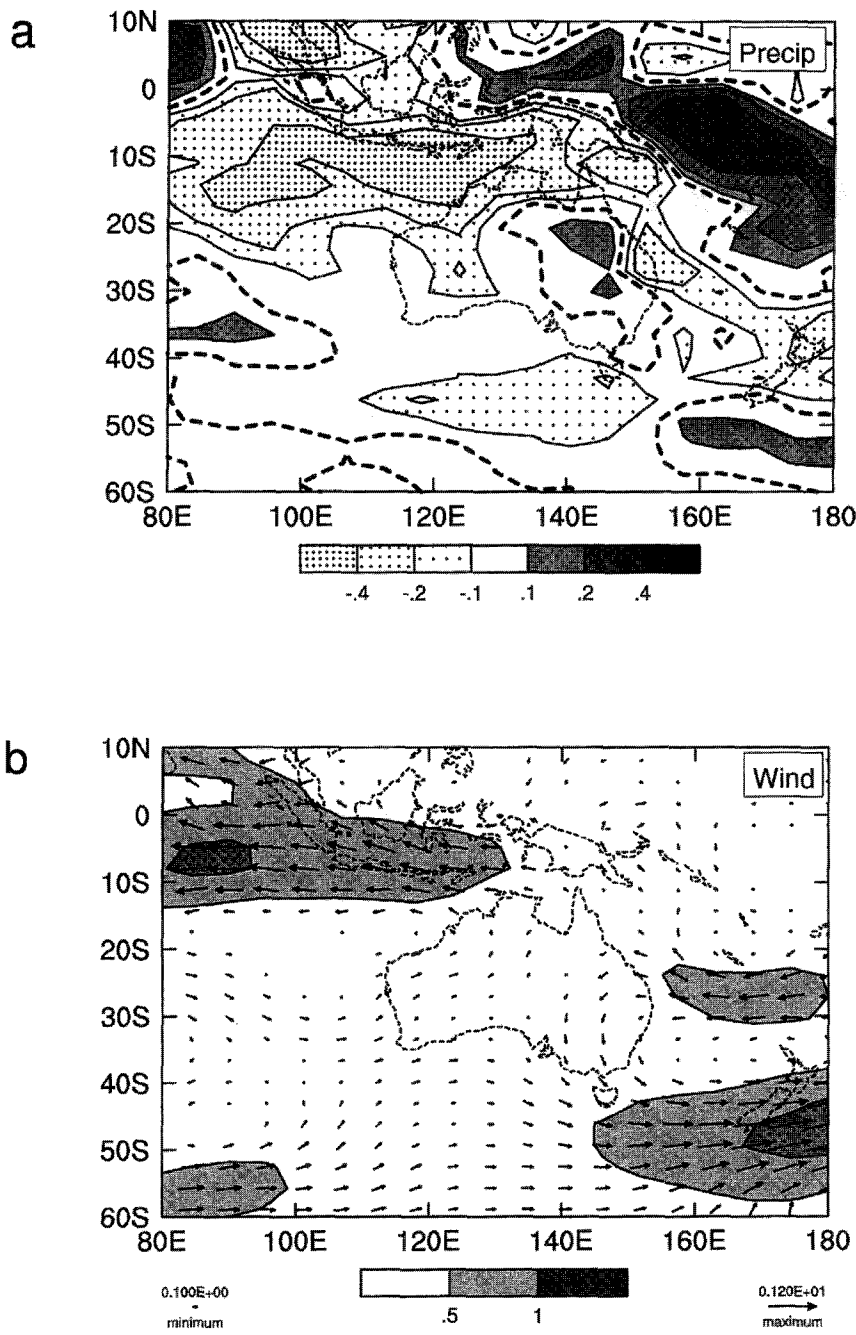


Figure 6a-b.

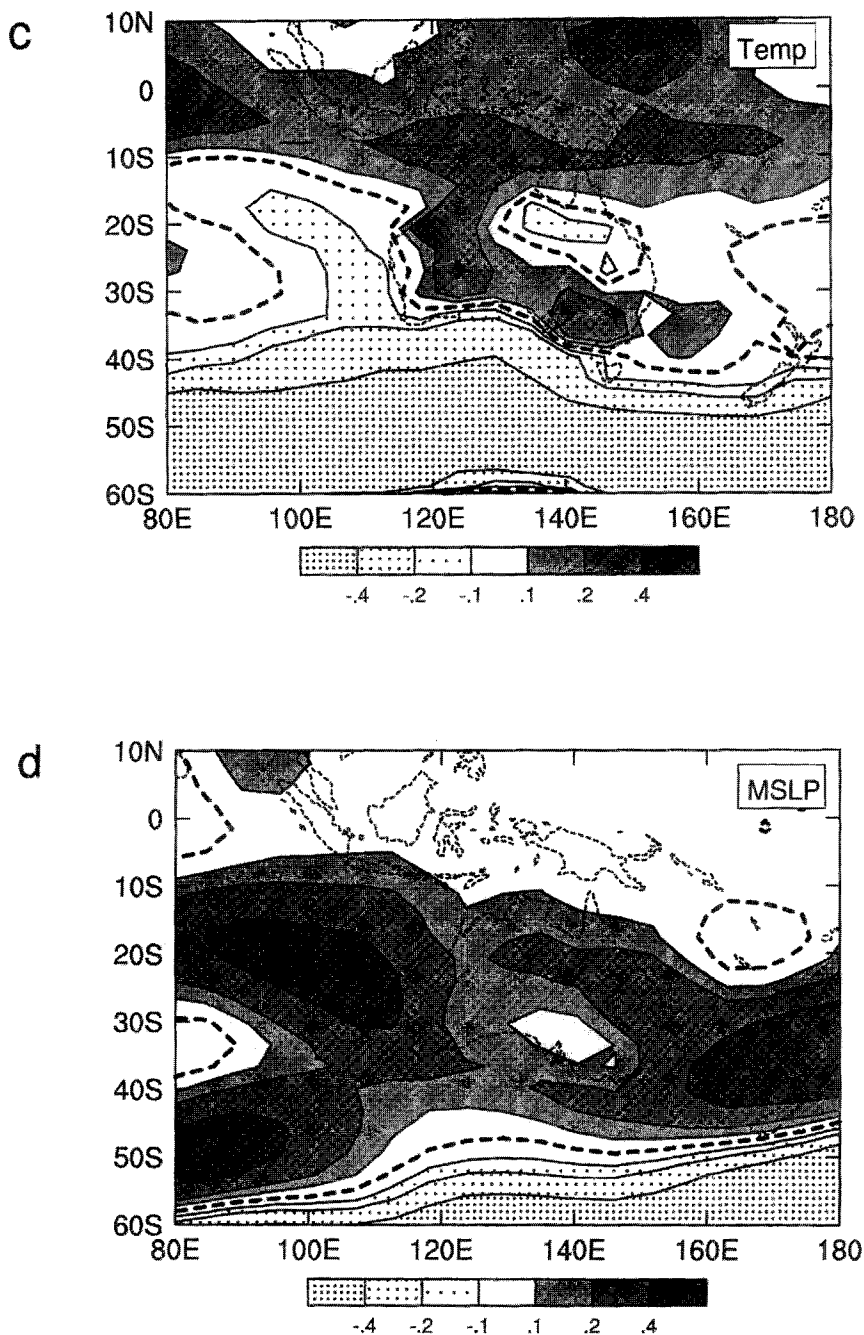


Figure 6c-d.

Figure 6. Difference between normalised DJF changes for enhanced greenhouse conditions in CSIROC (coupled experiment) and CSIROM (mixed layer experiment): (a) rainfall (mm/day), (b) vector wind at 807-hPa level (see scale in ms^{-1}), (c) surface temperature ($^{\circ}\text{C}$) and (d) MSL pressure (hPa).

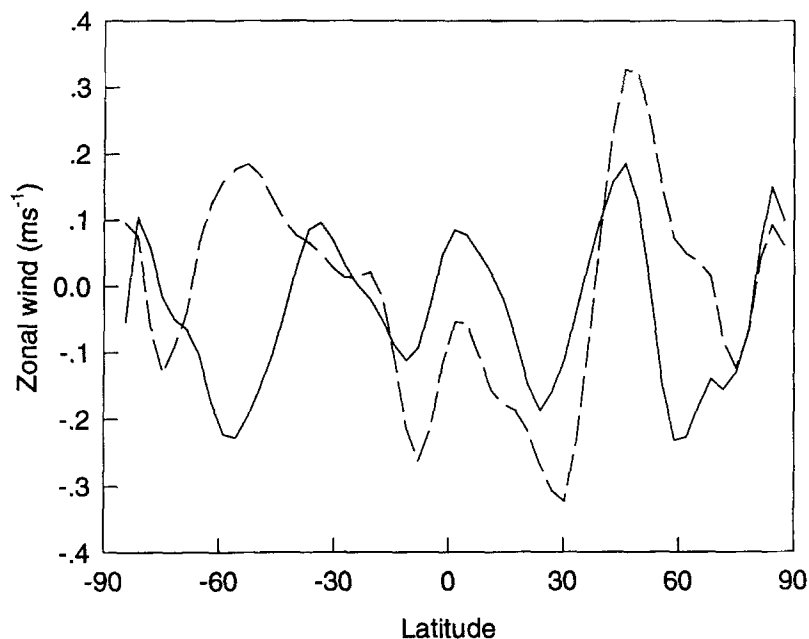


Figure 7. Normalised DJF change for enhanced greenhouse conditions in zonal wind at the 807 hPa level (ms^{-1}) averaged over all longitudes for CSIRO ROM (solid line) and CSIRO OC (dashed line). Note that a westerly wind anomaly is positive.

Oscillation (ENSO) variations (see Drosowsky, 1993). For example, summers with weaker monsoonal winds, strengthened subtropical high pressure in the eastern Indian Ocean, and reduced monsoonal rainfall occur in conjunction with El Niño signatures in the central and eastern Pacific. Such signatures, such as a westerly wind anomaly in the central Pacific, are not evident in the CSIRO coupled enhanced greenhouse experiment (analysis not shown). This suggests that changes in ENSO-related behaviour in the coupled experiment cannot be invoked to explain the rainfall differences in the CSIRO simulations.

5. How Reliable Are the Southern Hemisphere Results of Coupled GCMs?

The rainfall results above demonstrate that any regional climate-change scenarios prepared for Australia (and for the southern hemisphere more generally), could be very different depending on whether coupled or mixed layer ocean experiments are used. This need not be a problem if we have strong reasons for preferring the results of one type of experiment. Indeed, one could presume that in principle the results of coupled experiments are superior to those of mixed layer ocean experiments because the coupled ocean-atmosphere model formulation is a more complete representation of the climate system, and, unlike the mixed layer ocean experiments, these models can simulate changes in oceanic circulation in response

to enhanced greenhouse conditions. However, one has to be careful in making this presumption, as the ocean models used in climate-change experiments have yet to be extensively validated. From our perspective, it is vital to know how well the ocean models simulate the absorption of heat over the southern ocean. We now consider this point.

England et al. (1994) and England (1995) simulate oceanic uptake of atmospheric CFC-11 from 1930 to the present using a version of the GFDL ocean model. Comparison of the results with observed CFC-11 sections in the Southern Ocean showed that the model greatly overestimates local uptake of this neutral tracer gas. We present here the comparison of observed and modelled CFC-11 concentrations for a cross-section south of Australia (Figure 8). The cross-section runs from Tasmania southward to the Antarctic continent and was measured as part of the World Ocean Circulation Experiment (WOCE line SR3). This result indicates that the ocean model significantly overestimates vertical mixing and convective overturning south of 50° S (although it is a little underestimated north of this latitude). Furthermore the overestimate is more marked and extends further north in some other sections (e.g., see England, 1995). This suggests that the simulated uptake of heat in this region in certain coupled enhanced greenhouse experiments could also be too large. A similar version of the GFDL ocean model was used in the CSIROC, GFDLC and UKMOC coupled enhanced greenhouse experiments considered here. Although somewhat different ocean models are used in the MPILC and MPIOC, these experiments produce a very similar warming pattern to the other models (see Figure 5) which suggests that they too overestimate vertical mixing in the Southern Ocean.

To examine this issue further, we calculate the mixed layer depth, using a density step criterion in observations (Levitus, 1982) and in the CSIROC coupled model control experiment. Figure 9 shows the results for the late southern winter (September) when surface mixed layers are at their deepest. The observed mixed layer depths are mostly less than 200 m, except for a band around 45° S, including south of Australia, where depths can be in excess of 500 m. In the model, mixed layer depths are much greater than observations throughout the hemisphere south of around 40° S, and at 60° S quite unrealistic depths of 3000 m are present. Indeed, it could be argued that errors in the mixed layer depth in CSIROC are more serious than the errors associated with using a fixed mixed layer depth of 50 m, such as was done in the CSIROCM mixed layer experiment. At the very least, it would appear that the real behaviour of the ocean is likely to lie between these two model extremes.

In summary, these oceanographic results suggest that the pattern of warming in the southern hemisphere simulated in current coupled models could be misleading. Consequently, patterns of simulated rainfall change which are apparently linked to this pattern of warming could also be unreliable. As has been noted by England (1995), if the coupled models are in general sequestering heat too rapidly in the deep ocean, the transient rate of global atmospheric warming may at present be

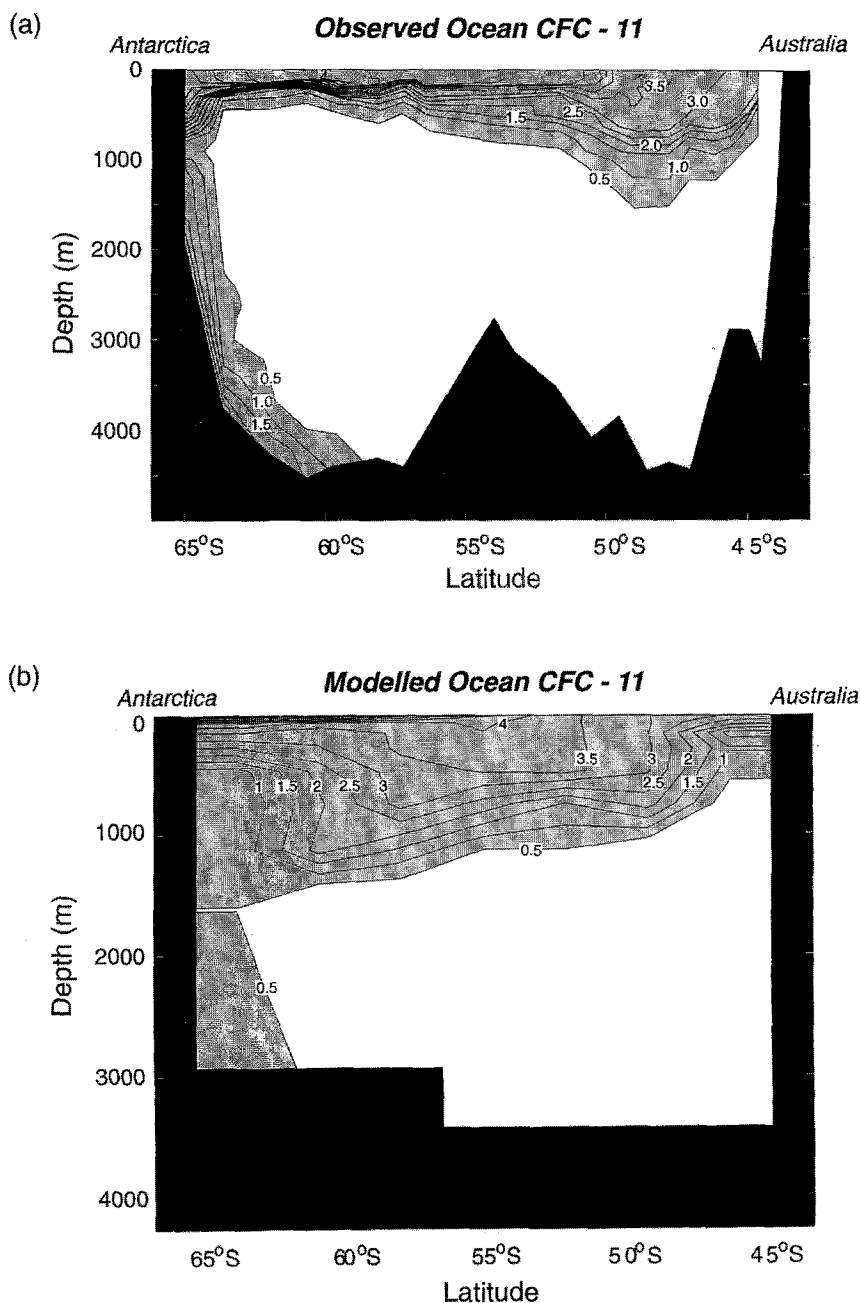


Figure 8. Latitude-depth sections of dissolved CFC-11 (pmol/kg): (a) observed along WOCE section SR3 (south of Australia) during September 1991 (provided courtesy of Dr. John Bullister of NOAA/PMEL), and (b) simulated for the corresponding cross section in an experiment using the GFDL ocean model (details of which are given in England et al., 1994). (Originally published in *Geophysical Research Letters* 22 (22), cover.)

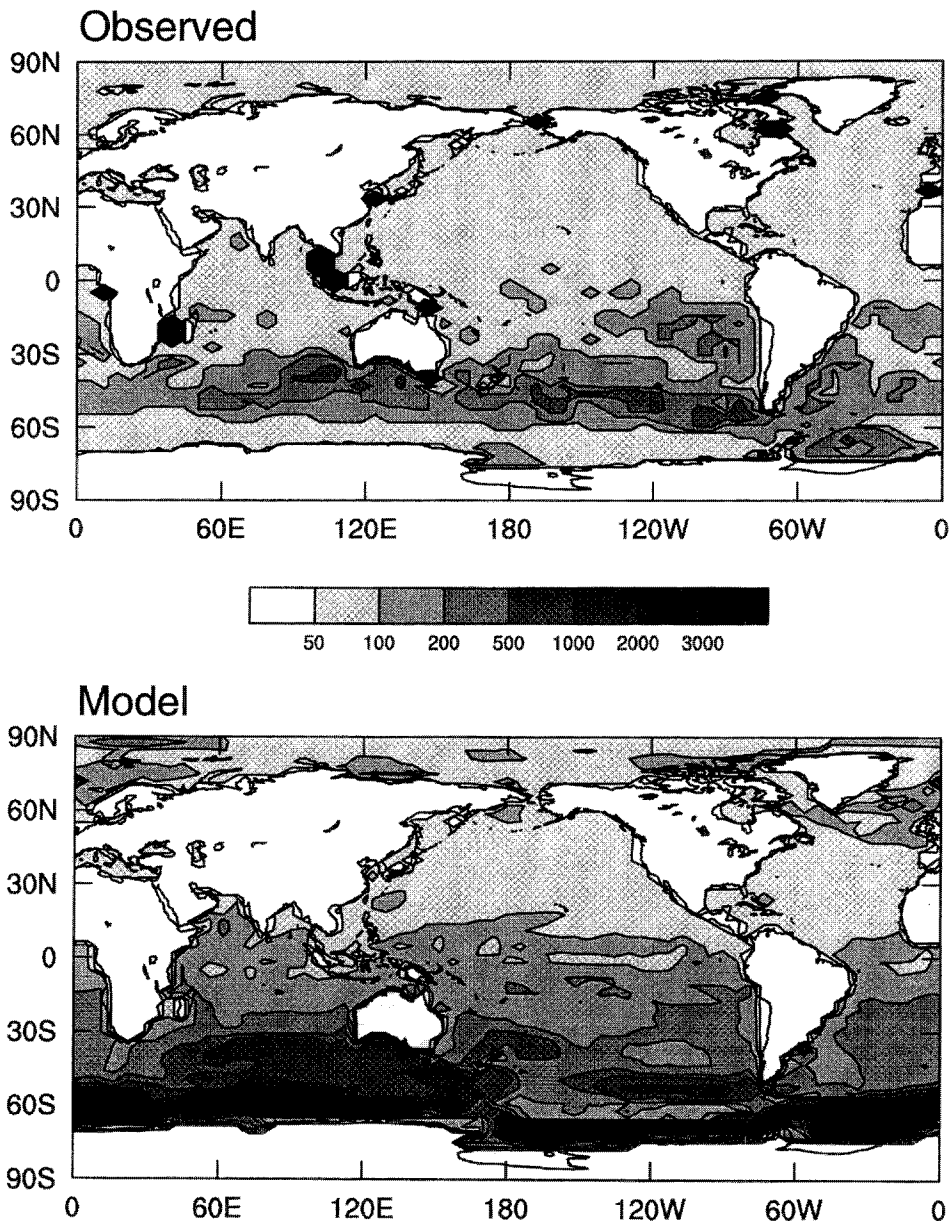


Figure 9. September mixed layer depth (in metres), calculated using a density step criterion for observations (Levitus, 1982), and the CSIROC coupled model control experiments. The mixed layer depth was identified as the location where a change of density greater than 0.3 kg/m^3 occurs between levels in the ocean model (twelve levels in total) and in observations (interpolated to the model grid).

underestimated in the coupled models. This has wider global significance. There are also likely to be important implications for global and regional rates of increase of mean sea level.

6. Concluding Discussion

Simulated patterns of precipitation change over the southern hemisphere, and especially in the Australian region, are quite different in recent coupled ocean enhanced greenhouse experiments from what they are in recent mixed layer ocean experiments. The difference is most marked in the southern summer when the mixed layer models simulate rainfall increases for a broad tropical to subtropical region centred on Australia, whereas the coupled models tend to simulate decreases for this region. Although the signal-to-noise ratio in simulated rainfall change at the regional scale is low (particularly in the coupled models), several factors point towards the difference being a systematic regional effect. First, the agreement on the simulated sign of rainfall change amongst the mixed layer and amongst the coupled models is considerably greater than that expected by chance. Secondly, the tendency for the coupled model results to differ markedly from the mixed layer experiments does not extend to the northern hemisphere. To a striking extent, both the coupled and mixed layer experiments agree on increased rainfall in the high latitudes (extending to the mid latitudes in winter) and in areas affected by the summer monsoon (e.g., India). Similarly there is strong agreement in both coupled and mixed layer models on decreasing rainfall over continental mid latitudes in summer (particularly over north America and southern Europe). Thirdly, the southern hemisphere differences in simulated rainfall can, at least in part, be related to the markedly different pattern of warming simulated in the coupled models for the southern hemisphere.

From the point of view of developing regional scenarios of rainfall change in the southern hemisphere, and especially for Australia, it clearly matters a great deal whether mixed layer or coupled experiments are used. The difference in the regional rainfall results of the two model types increases the importance of the oceanographic evidence of errors in current coupled model simulations of the Southern Ocean. Indeed, the evidence suggests these simulations may be overestimating the role of the Southern Ocean in moderating climate change, simulating erroneously deep mixed layers that are unseen in the observed climatology of the region. These deep mixed layers are very efficient moderators of climate change, since the ocean has an enormous capacity to store heat. The implication for regional climate-change scenario development in the southern hemisphere is that it may be too soon to dispense with the mixed layer ocean experiments (which in effect assume a shallow mixed layer) and use solely the results of current coupled experiments. At the very least, it is clear that developing a coupled model with a better validated and

more reliable ocean formulation is vital for scenario development in the southern hemisphere.

Acknowledgements

This work would not have been possible without the climate modelling work of Hal Gordon, Martin Dix and Leon Rotstayn at CSIRO. Malcolm Haylock assisted with the analysis and Ian Simmonds provided some very useful comments on the work. We are also grateful for GCM data generously provided by modellers at Australian Bureau of Meteorology Research Centre, Geophysical Fluid Dynamics Laboratory, Max Planck Institut für Meteorologie, the Hadley Centre of United Kingdom Meteorological Office and the Canadian Climate Centre. The work was partly supported by funds provided by the National Greenhouse Research Program and the Governments of New South Wales, Victoria, Western Australia, the Northern Territory and Queensland. The work contributes to the CSIRO Climate Change Research Program.

References

- Burgos, J. J., Ponce, H. F., and Molion, L. C. B.: 1991, 'Climate Change Predictions for South America', *Clim. Change* **18**, 223–239.
- Charlson, R. J., Langner, J., Rodhe, H., Leovy, C. B., and Warren, S. G.: 1991, 'Perturbation of the Northern Hemisphere Radiative Balance by Backscattering from Anthropogenic Sulfate Aerosols', *Tellus* **43AB**, 152–163.
- Chiew, F. H. S., Whetton, P. H., McMahon T. A., and Pittock A. B.: 1995, 'Simulation of the Impacts of Climate Change on Runoff and Soil Moisture in Australian Catchments', *J. Hydrology* **167**, 121–147.
- CIG: 1992, *Climate Change Scenarios for the Australian Region*, Climate Impact Group, CSIRO Division of Atmospheric Research, Melbourne, 6 pp.
- CLIVAR, 1995: First Session of the CLIVAR Dec-Cen Numerical Experimentation Group (CLIVAR NEG-2), Hamburg, Germany, 11–13 September 1995, *ICPO Publ. Ser. No. 1*, International CLIVAR Project Office, Hamburg, Germany.
- Cohen, S. J.: 1990, 'Bringing the Global Warming Issue Closer to Home: The Challenge of Regional Impact Studies', *Bull. Am. Meteorol. Soc.* **71**, 520–526.
- Colman, R. A., McAvaney, B. J., Fraser, J. R., and Power S. B.: 1994, 'Annual Mean Meridional Energy Transport Modelled by a General Circulation Model for Present and $2 \times \text{CO}_2$ Equilibrium Climates', *Clim. Dynamics* **10**, 221–229.
- Cubasch, U., Hasselmann, K., Hock, H., Maier-Reimer, E., Mikolajewicz, U., Santer, B. D., and Sausen, R.: 1992, 'Time Dependent Greenhouse Warming Computations with a Coupled Ocean Atmosphere Model', *Clim. Dynamics* **8**, 55–69.
- Drosowsky, W.: 1993, 'An Analysis of Australian Seasonal Rainfall Anomalies: 1950–1987, II. Temporal Variability and Teleconnection Patterns', *Int. J. Climatol.* **13**, 111–149.
- England, M. H., Garcon, V., and Minster, J.: 1994, 'Chlorofluorocarbon Uptake in a World Ocean Model, 1. Sensitivity to the Surface Gas Forcing', *J. Geophys. Res.* **99**, 25, 215–225, 233.
- England, M. H.: 1995, 'Using Chlorofluorocarbons to Assess Ocean Models', *Geophys. Res. Letts.* **22**, 3051–3054.
- Gordon, H. G. and O'Farrell, S. P.: 1996, 'Transient Climate Change in the CSIRO Coupled Model and Dynamic Sea Ice', *Monthly Weather Review* in press.

- Gregory, J. M. and Mitchell, J. F. B.: 1995, 'Simulation of Daily Variability of Surface Temperature and Precipitation over Europe in the Current and $2 \times \text{CO}_2$ Climates using the UKMO High-Resolution Climate Model', *Q. J. Roy. Meteorol. Soc.* **121**, 1451–1476.
- Grotch, S. L. and MacCracken, M. C.: 1991, 'The Use of General Circulation Models to Predict Regional Climate Change', *J. Climate* **4**, 286–303.
- IPCC: 1990, Houghton, J. T., Jenkins, G. J., and Ephraums, J. J. (eds.), *Climate Change: The IPCC Scientific Assessment*, Cambridge University Press, Cambridge, 365 pp.
- IPCC: 1992, Houghton, J. T., Callander, B. A., and Varney, S. K. (eds.), *Climate Change 1992: The Supplementary Report to the IPCC Scientific Assessment*, Working Group 1, Cambridge University Press, Cambridge, 200 pp.
- Kellogg, W. W. and Zhao, Z.-C.: 1988, 'Sensitivity of Soil Moisture to Doubling of Carbon Dioxide in Climate Model Experiments, Part I: North America', *J. Climate* **1**, 348–366.
- Kowalczyk, E. A., Garratt, J. R., and Krummel, P. B.: 1991, 'A Soil-Canopy Scheme for Use in a Numerical Model of the Atmosphere – 1D Stand-Alone Model', *CSIRO Div. Atmos. Res. Tech. Pap.* No. 23, CSIRO, Melbourne, 56 pp.
- Legates, D. R. and Willmott, C. J.: 1990, 'Mean Seasonal and Spatial Variability in Gauge-Corrected, Global Precipitation', *Int. J. Climatol.* **10**, 111–127.
- Levitus, S.: 1982, *Climatological Atlas of the World Ocean*, NOAA Prof. Paper No. 13, U.S. Dept. of Commerce, Washington, DC, 173 pp.
- Lunkeit, F., Sausen, R., and Oberhuber, J. M.: 1994, 'Climate Simulations with the Global Coupled Atmosphere-Ocean Model ECHAM/OPYC, Part I: Present-Day Climate and ENSO Events', *MPI Report No. 132*, Max-Planck-Institute, Hamburg.
- McFarlane, N. A., Boer, G. J., Blanchet, J.-P., and Lazare, M.: 1992, 'The Canadian Climate Centre Second-Generation General Circulation Model and its Equilibrium Climate', *J. Climate* **5**, 1013–1044.
- Manabe, S., Stouffer, R. J., Spelman, M. J., and Bryan, K.: 1991, 'Transient Responses of a Coupled Ocean Atmosphere Model to Gradual Changes of Atmospheric CO_2 , Part I: Annual Mean Response', *J. Climate* **4**, 785–818.
- Mitchell, J. F. B., Johns, T. C., Gregory, J. M., and Tett, S. F. B.: 1995, 'Climate Responses to Increasing Levels of Greenhouse Gases and Sulphate Aerosols', *Nature* **376**, 501–504.
- Murphy, J. M.: 1995, 'Transient Response of the Hadley Centre Coupled Ocean-Atmosphere Model to Increasing Carbon Dioxide, Part I: Control Climate and Flux Adjustment', *J. Climate* **8**, 36–56.
- Murphy, J. M. and Mitchell, J. F. B.: 1995, 'Transient Response of the Hadley Centre Coupled Ocean-Atmosphere Model to Increasing Carbon Dioxide, Part II: Spatial and Temporal Structure of Response', *J. Climate* **8**, 57–80.
- O'Farrell, S. P.: 1996, 'Sensitivity Study of a Dynamical Ice Model; the Effect of the External Stresses and Land Boundary Conditions on Ice Thickness Distribution', *J. Geophys. Res.* in press.
- Parry, M. L., Kenny, G. J., and Harrison, P. A.: 1993, 'Aims and Methods', in Kenny, G. J., Harrison, P. A., and Parry, M. L. (eds.), *The Effect of Climate Change on Agricultural and Horticultural Potential in Europe*, Research Report No. 2, Environmental Change Unit, University of Oxford, Oxford, pp. 1–11.
- Rowntree, P. R.: 1990, 'Estimates of Future Climatic Change over Britain', *Weather* **45**, 79–89.
- Taylor, K. E. and Penner, J. E.: 1994, 'Response of the Climate System to Atmospheric Aerosols and Greenhouse Gases', *Nature* **369**, 734–737.
- Washington, W. M. and Meehl, G. A.: 1989, 'Climate Sensitivity due to Increased CO_2 : Experiments with a Coupled Atmosphere and Ocean General Circulation Model', *Clim. Dynamics* **4**, 1–38.
- Watterson, I. G., Dix, M. R., Gordon, H. B., and McGregor, J. L.: 1995, 'The CSIRO 9-level Atmospheric General Circulation Model and Its Equilibrium Present and Doubled CO_2 Climates', *Aust. Met. Mag.* **44**, 111–125.
- Whetton, P. H.: 1996, Comment on 'Global and Terrestrial Precipitation: A Comparative Assessment of Existing Climatologies' by D. R. Legates, *Int. J. Climatol.* in press.
- Whetton, P. H., Fowler, A. M., Haylock, M. R., and Pittock, A. B.: 1993, 'Implications of Climate Change due to the Enhanced Greenhouse Effect on Floods and Droughts in Australia', *Clim. Change* **25**, 289–317.

- Whetton, P. H., Haylock, M. R., and Galloway, R.: 1996a, 'Climate Change and Snow Cover Duration in the Australian Alps, *Clim. Change* **32**, 447–479.
- Whetton, P. H., Pittock, A. B., Labraga, J. C., Mullan, A. B., and Joubert, A., 1996b, in Henderson-Sellers, A. and Giambelluca, T. (eds.), *Climate Change, People and Policy: Developing Southern Hemisphere Perspectives*, Wiley, Chichester, pp. 89–130.
- Wigley, T. M. L. and Raper, S. C. B.: 1992, 'Implications for Climate and Sea-Level of Revised IPCC Emissions Scenarios', *Nature* **357**, 293–300.
- Zhao, Z.-C., and Kellogg, W.W.: 1988, 'Sensitivity of Soil Moisture to Doubling of Carbon Dioxide in Climate Model Experiments, Part II: The Asian Monsoon Region', *J. Climate* **1**, 367–378.

(Received 17 July 1995; in revised form 16 April 1996)